ORIGINAL ARTICLE

AASLD
AMERICAN ASSOCIATION FOR
THE STUDY OF LIVER DISEASES

Proteomics-based identification of the role of osteosarcoma amplified-9 in hepatocellular carcinoma recurrence

Xuyong Wei[1,2,3] | Mengfan Yang[1,2,3,4] | Binhua Pan[1,2,3,4] | Xiaobing Zhang[1,2,3] | Hanchao Lin[1,2,3] | Wangyao Li[1,2,3] | Wenzhi Shu[1,2,3] | Kun Wang[1,2] | Abdul Rehman Khan[1,2,3,4] | Xuanyu Zhang[3,4] | Beini Cen[1,2,3] | Xiao Xu[1,2,3,4,5,6] (iD)

[1]Department of Hepatobiliary and Pancreatic Surgery, Affiliated Hangzhou First People's Hospital, Zhejiang University School of Medicine, Hangzhou, China

[2]Key Laboratory of Integrated Oncology and Intelligent Medicine of Zhejiang Province, Hangzhou, China

[3]NHC Key Laboratory of Combined Multi-Organ Transplantation, Hangzhou, China

[4]Department of Hepatobiliary and Pancreatic Surgery, The First Affiliated Hospital, Zhejiang University School of Medicine, Hangzhou, China

[5]Zhejiang University Cancer Center, Hangzhou, China

[6]Institute of Organ Transplantation, Zhejiang University, Hangzhou, China

Correspondence
Xiao Xu, Department of Hepatobiliary and Pancreatic Surgery, Affiliated Hangzhou First People's Hospital, Zhejiang University School of Medicine, Hangzhou, China.
Email: zjxu@zju.edu.cn

Abstract

Hepatocellular carcinoma (HCC) is one of the most prevalent malignancies; its recurrence is associated with high mortality and poor recurrence-free survival and is affected by multisystem and multilevel pathological changes. To identify the key proteins associated with tumor recurrence and the underlying mechanisms, proteomic profiling of tumor specimens from early recurrence and nonrecurrence patients was performed in this study. Proteomics was applied to identify differentially expressed proteins during the early recurrence of HCC after surgery. Osteosarcoma amplified-9 (OS-9) was discovered, and the correlation between OS-9 expression and the clinicopathological characteristics of patients was analyzed. Invasion and migration were examined in SMMC-7721 cells with and without OS-9 overexpression. Proteomics was performed once again using SMMC-7721 cells with OS-9 overexpression to further analyze the proteins with altered expression. OS-9 was overexpressed in the early recurrence group, and OS-9 overexpression was associated with high serum alpha-fetoprotein levels and poor recurrence-free survival in 196 patients with HCC. The invasion and migration abilities of SMMC-7721 cells were enhanced in the OS-9 overexpression group. Bioinformatic functional enrichment methods, including Gene Ontology annotation and Kyoto Encyclopedia of Genes and Genomes pathway analysis, revealed that the hypoxia-inducible factor 1 (HIF-1) and tumor necrosis factor (TNF) signaling pathways were activated in the OS-9 overexpression group. The migration and invasion capacities of OS-9 overexpressed HCC cell line were weakened while treated with HIF-1α or TNF-α inhibitors. *Conclusion:* Our results suggest that the overexpression of OS-9 is related to HCC recurrence, thereby

---

Xuyong Wei and Mengfan Yang contributed equally to this work.

contributing to the migration and invasion capacities of HCC cell line by regulating the HIF-1 and TNF pathways.

INTRODUCTION

Hepatocellular carcinoma (HCC) is one of the most prevalent malignancies; its prevalence has been increasing rapidly, by 2%–3% annually, over the past decade, although the pace has slowed in recent years.[1,2] Moreover, HCC is a leading cause of cancer-related mortality, with a 5-year overall survival rate of 18% for all stages combined.[1] Surgical resection remains the mainstay of curative therapy for HCC at an early stage. The overall survival rate after surgery remains low, due to the high incidence of early recurrence despite the advancement of diagnostic procedures and treatments. Various studies have revealed that almost 70% of patients develop recurrence within 5 years after resection.[3–5] The underlying molecular pathological mechanism of HCC recurrence has not been fully explored and needs to be studied urgently to improve the prognosis after surgery.

Osteosarcoma amplified-9 (OS-9) was first identified by Su et al. and was shown to be amplified and overexpressed in human sarcoma specimens.[6] Similar effects of OS-9 were confirmed in myeloid leukemia in 1998.[7] However, the negative form of OS-9 has been shown in other tumors.[8,9] Additionally, OS-9 interacts with hypoxia-inducible factor 1α (HIF-1α), promotes the oxygen-dependent degradation of HIF-1α, and ultimately reduces the transcriptional activity and expression of HIF-1α, which impairs tumor growth and metastasis.[8–10]

In this study, we investigated the protein OS-9 in the tumor tissues of patients and its relationship with HCC recurrence based on proteomics. Furthermore, the underlying mechanism of OS-9 and HCC recurrence was explored by secondary proteomics.

METHODS

Clinical materials and sample preparation

All clinical samples were collected from patients with HCC who underwent hepatectomy at the First Affiliated Hospital, College of Medicine, Zhejiang University, between 2014 and 2015. Three pairs of samples from patients with early recurrence (<24 months) and nonrecurrence (cryopreserved at −80°C) were used for proteomic profiling, and another 196 samples of HCC tissues were formalin-fixed and paraffin-embedded for immunohistochemical (IHC) analysis. All specimens had an individual hospital ID number, and information regarding clinicopathological characteristics, including age, sex, tumor size, lymph node invasion, distant metastasis, alpha-fetoprotein (AFP) level, differentiation degree, and follow-up prognosis, was collected and recorded in detail. This study was performed according to the protocols approved by the Research Medical Ethical Committee of the First Affiliated Hospital, School of Medicine, Zhejiang University.

Proteomic analysis and database search

The protein solution was reduced for 30 min and alkylated for 15 min for digestion. The protein sample was diluted with 100 mM Triethylamonium bicarbonate. Finally, trypsin was added at a 1:50 trypsin-to-protein mass ratio for the first digestion overnight and a 1:100 ratio for the second 4-hours digestion.

The tryptic peptides were dissolved in formic acid and directly loaded onto a homemade reversed-phase analytical column. The peptides were subjected to a nanospray ion source followed by tandem mass spectrometry (MS-MS) in Q Exactive Plus (Thermo Fisher Scientifc). Peptides were then selected for MS-MS, and the fragments were detected. A data-dependent procedure that alternated between one MS scan followed by 20 MS-MS scans with a 15.0-s dynamic exclusion was used.

The resulting MS data were processed using the MaxQuant search engine (v.1.6.6.0). Tandem mass spectra were searched against the human UniProt database concatenated with a reverse decoy database. The false discovery rate was adjusted to <1%, and the minimum score for modified peptides was set at >40.

IHC staining

IHC staining was performed with formalin-fixed and paraffin-embedded 196 HCC tissues sectioned to a thickness of 4 μm. The slides were placed in an ethylenediaminetetraacetic acid buffer for antigen repair. Forty microliters of diluted primary antibody (1:1000, ab19853; Abcam) was added to the slide and incubated for 30 min at room temperature. The slides were then treated with a secondary antibody for 60 min at room temperature. 3,3′-Diaminobenzidine was used as the chromogenic substrate. Tumor tissues stained for the OS-9 protein were scored using the histochemistry score, which was further used to transform the number of positive cells and their staining intensity in each section into corresponding values to achieve semi-quantitative analysis.

Finally, the median score was regarded as the cutoff and divided into high or low expression.

Cell culture

HCC cell lines SMMC7721 were obtained from the Cell Bank of the Chinese Academy of Sciences (Shanghai, China). SMMC7721 cells were cultured in Roswell Park Memorial Institute 1640 medium supplemented with 10% FBS. All cell lines were cultured at 37°C in a 5% carbon dioxide incubator.

Protein extraction

Cell samples were sonicated three times on ice using a high-intensity ultrasonic processor (Scientz), in lysis buffer (8 M urea, 1% protease inhibitor cocktail), after being washed three times with precooled phosphate-buffered saline (PBS). The supernatants were collected via centrifugation for 10 min. The proteins were quantified using the BCATM Protein Assay Kit (Beyotime) and stored at −80°C.

Western blot analysis

Equal amounts of protein samples were separated via sodium dodecyl sulfate-polyacrylamide gel electrophoresis and transferred onto polyvinylidene difluoride membranes (Millipore). After blocking with 5% blocking reagent for 1 hour, the membranes were incubated with primary antibodies against OS-9 (1:1000, ab19853; Abcam), HIF-1α (1:1000, ab179483; Abcam), and beta actin (1:5000, ab6276; Abcam) at 4°C overnight. After washing with Tris-buffered saline containing 0.1% Tween 20, the membranes were incubated for 2 hours with horseradish peroxidase-coupled anti-rabbit immunoglobulin G (1:2500, ab6721; Abcam) at room temperature. Densitometry analysis of protein bands was performed using the Millipore ECL Western Blot Analysis Substrate (Merck Millipore). All bands were analyzed using the ImageJ software (Version 2.1.0; National Institutes of Health).

Cell transfection

Cell transfection was performed using Lipofectamine 3000 (Invitrogen) following the manufacturer's instructions. SMMC7721 cells were cultured and uniformly inoculated into 96-well plates at 1×10^4/well. Lentiviruses OS-9 overexpressing lentiviral vectors (Hanbio Biotechnology Co., Ltd.) and controls were purchased. SMMC7721 cells (2×10^4/well) were transiently transfected with lentiviral vectors and collected 24 hours following transfection. The cells with stably depleted expression and overexpression of OS-9 were selected by culturing in a medium containing penicillin and streptomycin. The efficiency of transduction was confirmed with western blotting.

Tumor invasion and migration assay

A polycarbonate membrane Transwell (Corning) and Matrigel (BD) were used for the migration assay. Cells were starved for 24 hours before the suspension, lysed, and washed with PBS before being resuspended in serum-free media. In total, 2×10^5 SMMC7721 cells for both OS-9 overexpression and control groups were suspended in 200 μl of serum-free medium and seeded into the upper chamber, while 600 μl of DMEM containing 10% FBS was added to the lower chamber. After incubation for 48 hours at 37°C, the remaining cells on the upper surface were removed. The invading cells were fixed in methanol and stained with 0.5% crystal violet. Cells on the lower surface of the membrane were counted in randomly selected fields under a microscope (Olympus). The experiment was repeated 3 times independently.

In the migration experiment, all of the steps were the same as those in the invasion experiment, except that Matrigel was not used in the upper chamber.

Reverse-transcription polymerase chain reaction for messenger RNA analysis

Total RNA was extracted from SMMC-7721 cells overexpressing OS-9 and control cells using 1 ml of TRIzol reagent (Invitrogen). Quantitative real-time polymerase chain reaction (PCR) was carried out using ABI Prism 7500 Fast Sequence Detection System (Applied Biosystems) and DNA Master SYBR Green Kit (Takara Bio, Japan) according to the manufacturer's instructions. The specific primer pairs used for the target genes are listed in Table 1. The PCR reaction conditions were as follows: 40 cycles of denaturation at 95°C for 30 s, annealing at 95°C for 10 s, and extension at 60°C for 30 s. All reactions were performed in triplicate. The expression values were calculated using the $2^{-\Delta\Delta Ct}$ method, and all results were normalized to the messenger RNA (mRNA) expression of glyceraldehyde 3-phosphate dehydrogenase, which was used as an internal control.

Bioinformatic methods

Proteins were classified by Gene Ontology (GO) annotation into the following three categories:

TABLE 1 Forward and reverse primers of genes for real-time polymerase chain reaction amplification

Primers		Sequence
GAPDH	Forward	GGTGGTCTCCTCTGACTTCAACA
GAPDH	Reverse	GTTGTAGCCAAATTCGTTGT
ENO1	Forward	CCTGCCCTGGTTAGCAAGAA
ENO1	Reverse	GGCGTTCGCACCAAACTTAG
ENO2	Forward	CGTTACTTAGGCAAAGGTGTCC
ENO2	Reverse	CTCCAGCATCAGGTTGTCCAGT
LDHA	Forward	CAAGAGGTACCACTGCCCAT
LDHA	Reverse	CACCTTGGCTAAAGGAACCA
TNF-α	Forward	CCAGAGGGAAGAGCAGTCCC
TNF-α	Reverse	TCGGCTACAACGTGGGCTAC
ALDOA	Forward	TCATCCTCTTCCATGAGACACTCT
ALDOA	Reverse	ATTCTGCTGGCAGATACTGGCATAA
ENO3	Forward	TATCGCAATGGGAAGTACGATCT
ENO3	Reverse	AAGCTCTTATACAGCTCTCCGA
MLKL	Forward	AGGAGGCTAATGGGGAGATAGA
MLKL	Reverse	TGGCTTGCTGTTAGAAACCTG
TNFAIP3	Forward	TGCTGCCCTAGAAGTACAATAGGAA
TNFAIP3	Reverse	GCAGCTGGTTGAGTTTATGCAAG
JUNB	Forward	CTTCTACCACGACGACTCATAC
JUNB	Reverse	TTTCAGGAGTTTGTAGTCGTGT
CASP7	Forward	TGCAAAGCCAGACAGAAGTAG
CASP7	Reverse	GGTCCATCGGTGCCATAAAT
TRAF5	Forward	GGATGAAACCACAGGGCATA
TRAF5	Reverse	GCAGCCAGGAGCAGCAG

biological process, cellular compartment, and molecular function. The Kyoto Encyclopedia of Genes and Genomes (KEGG) database was used to identify enriched pathways. These pathways were classified into hierarchical categories according to the KEGG website. For each category of proteins, the InterPro database and a two-tailed Fisher's exact test were used to test the enrichment of the differentially expressed proteins against all of the identified proteins.

For hierarchical clustering based on differentially expressed protein functional classifications, we first collated all categories obtained after enrichment, along with their p values, and then filtered for the categories that were enriched in at least one of the clusters. This filtered p value matrix was transformed by the function $x = -\log_{10}(p$ value$)$. Finally, the x values were z-transformed for each functional category. These z scores were then clustered using a one-way hierarchical clustering in Genesis. Cluster membership was visualized with a heat map using the "heatmap.2" function in the "gplots" R-package.

All differentially expressed protein database accessions or sequences were searched against the STRING database (version 10.1) for protein–protein interactions. Only interactions between the proteins belonging to the searched data set were selected, thereby excluding external candidates. STRING defines a metric termed "confidence score" to define interaction confidence; all interactions that were fetched had a confidence score ≥ 0.7 (high confidence). The interaction network from STRING was visualized in the R package "networkD3."

Inhibition of signaling proteins interplay with OS-9

Inhibitors including HIF-1α and tumor necrosis factor alpha (TNF-α) were obtained (VH-298, MedChemExpress; HY-100947, Methylthiouracil; HY-B0513, MedChemExpress). OS-9 overexpression or control SMMC-7721 were treated with the two inhibitors at 20 μM or 20 μM, respectively, and then invasion and migration assay were administrated.

Statistical analysis

The SPSS software (version 23.0; SPSS) was used for data analysis. Measurement data are presented as mean ± SD, and a t-test was used for intergroup comparisons. A χ^2 test was used for intergroup comparisons of count data; Fisher's exact test was used when the sample size was less than 5. The postoperative recurrence-free and overall survival rates were expressed using Kaplan-Meier curves, and the log-rank χ^2 test was used for comparisons between high and low expression groups. Multivariate Cox regression analysis was used to analyze the recurrence-free survival rate. All statistical tests were bilateral, and statistical significance was set at $p < 0.05$.

RESULTS

Proteomics was applied to discover differentially expressed proteins during the early recurrence of HCC after surgery

Among all the 3723 proteins, 17 were up-regulated in the HCC tissues from patients with early recurrence (n = 3), while 18 were up-regulated in the tissues of matched patients with nonrecurrence ($p < 0.05$) (Figure 1). All 35 proteins with expression changes greater than 1.5-fold were analyzed (Table 2). The change in OS-9 expression exceeded 300-fold and was largest among all proteins.

TABLE 2 Thirty-five unique proteins (>1.5-fold change and *p* value < 0.05) were identified between early recurrence and nonrecurrence patients

Accession	Protein name	Ratio	Regulated type	*p* value
63252870	Protein OS-9 isoform 4 precursor	344.984	Up	0.002
20149496	EF-hand domain-containing protein D1 isoform 1	1.989	Up	0.008
28976154	Trafficking protein particle complex subunit 6B isoform 2	1.923	Up	0.014
208879470	Eukaryotic translation elongation factor 1 epsilon-1 isoform 2	1.742	Up	0.017
530405632	E3 ubiquitin-protein ligase ARIH1 isoform X1	1.732	Up	0.046
295986608	Immunoglobulin lambda-like polypeptide 5 isoform 1	1.721	Up	0.028
5174411	CD5 antigen-like precursor	1.679	Up	0.016
399788586	Negative elongation factor C/D	1.664	Up	0.001
530391089	Tenascin isoform X4	1.654	Up	0.012
530411127	Bleomycin hydrolase isoform X1	1.627	Up	0.021
88900491	Neutral alpha-glucosidase AB isoform 3 precursor	1.625	Up	0.041
5032057	Protein S100-A11	1.581	Up	0.045
530398611	Chromodomain-helicase-DNA-binding protein 4 isoform X1	1.575	Up	0.009
4504349	Hemoglobin subunit beta	1.574	Up	0.028
530373812	Cohesin subunit SA-1 isoform X1	1.532	Up	0.007
530427497	Unconventional myosin-If isoform X2	1.517	Up	0.034
258679498	Carbonic anhydrase 1	1.505	Up	0.036
530366108	Conserved oligomeric Golgi complex subunit 2 isoform X1	−1.504	Down	0.019
8051636	Exportin-T	−1.512	Down	0.013
355390315	Protein scribble homolog isoform b	−1.535	Down	0.008
300244569	Serine/arginine-rich splicing factor 11 isoform 2	−1.602	Down	0.005
171460928	1,2-dihydroxy-3-keto-5-methylthiopentene dioxygenase	−1.604	Down	0.01
4504505	Peroxisomal multifunctional enzyme type 2 isoform 2	−1.621	Down	0.033
4557481	Canalicular multispecific organic anion transporter 1	−1.657	Down	0.005
24586679	Histone H2B type 1-A	−1.674	Down	0.047
530395424	Solute carrier family 22 member 18 isoform X2	−1.802	Down	0.011
530425831	Ral GTPase-activating protein subunit alpha-2 isoform X2	−1.804	Down	0.047
11068137	Hydroxyacid oxidase 1	−1.885	Down	0.04
548923675	2-hydroxyacyl-CoA lyase 1 isoform d	−2.003	Down	0.017
530362126	Fatty-acid amide hydrolase 1 isoform X1	−2.007	Down	0.023
530386343	Transferrin receptor protein 2 isoform X1	−2.153	Down	0.022
4503987	Gamma-glutamyl hydrolase precursor	−2.19	Down	0.003
530402736	Conserved oligomeric Golgi complex subunit 3 isoform X6	−2.343	Down	0.025
55770895	Protein LAP2 isoform 7	−2.71	Down	0.027
116875826	HD domain-containing protein 2	−246.486	Down	0.008

OS-9 expression was correlated with some clinicopathological features in patients with HCC

The patients were equally divided into a low OS-9 expression group (n = 98) and a high OS-9 expression group (n = 98) based on the median expression levels of OS-9 as the cutoff value in IHC analysis. Representative IHC results are shown in Figure 2A–D. The correlations between OS-9 expression and the clinicopathological characteristics of patients with HCC were analyzed using the chi-square test (Table 3). The serum AFP levels of patients were higher in the high OS-9 expression group than in the low OS-9 expression group ($p < 0.05$). The high OS-9 expression group showed a higher rate of HCC recurrence than the low OS-9 expression group ($p < 0.001$) (Figure 2E,F). However, OS-9 expression did not significantly differ by age, sex, hepatitis B virus infection, tumor size, histological differentiation, vascular invasion, or the number of tumors.
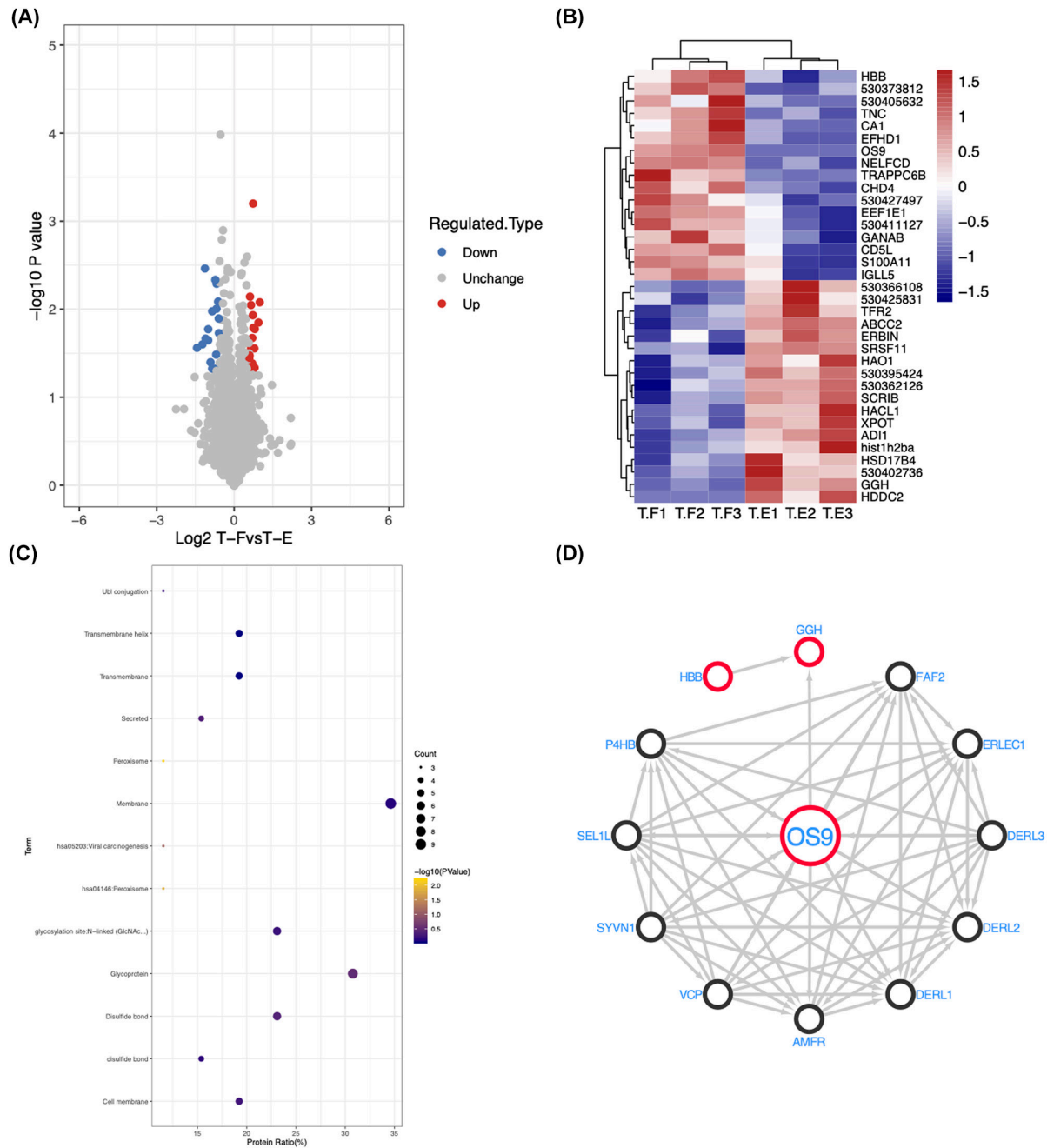
FIGURE 1 Differential proteins expression in early recurrence group (n = 3) and non–early recurrence group (n = 3). (A) Volcano plot of the differentially expressed proteins. Gray dots represent genes that are not differentially expressed in the early recurrence group and non–recurrence group; red dots and blue dots represent genes that are up-regulated and down-regulated significantly in early recurrence group. (B) Heat map of the differentially expressed proteins. Red rectangles mean that genes are up-regulated in these samples, and blue ones mean down-regulated. (C) Kyoto Encyclopedia of Genes and Genomes pathway enrichment for differentially expressed proteins. The sizes of the circle represent the number of genes enriched in pathways, and the color of the circle means significance. (D) Protein–protein interaction network of differentially expressed proteins with osteosarcoma amplified-9 (OS-9); the combined score of interactions are more than 0.4. Abbreviations: ABCC2, ATP binding cassette subfamily C member 2; ADI1, acireductone dioxygenase 1; AMFR, autocrine motility factor receptor; CA1, carbonic anhydrase 1; CD5L, CD5 molecule like; CHD4, chromodomain helicase DNA binding protein 4; DERL2, derlin 2; DERL3, derlin 3; DREL1, derlin 1; EEF1E1, eukaryotic translation elongation factor 1 epsilon 1; EFHD1, EF-hand domain family member D1; ERBIN, erbb2 interacting protein; ERLEC1, endoplasmic reticulum lectin 1; FAF2, Fas associated factor family member 2; GANAB, glucosidase II alpha subunit; GGH, gamma-glutamyl hydrolase; HACL1, 2-hydroxyacyl-CoA lyase 1; HAO1, hydroxyacid oxidase 1; HDDC2, HD domain containing 2; HIST1H2BA, histone cluster 1, H2ba; HSD17B4, hydroxysteroid 17-beta dehydrogenase 4; IGLL5, immunoglobulin lambda like polypeptide 5; NELFCD, negative elongation factor complex member C/D; OS-9, osteosarcoma amplified-9; P4HB, prolyl 4-hydroxylase subunit beta; S100A11, S100 calcium binding protein A11; SCRIB, scribble planar cell polarity protein; SEL1L, SEL1L adaptor subunit of ERAD E3 ubiquitin ligase; SRSF11, serine and arginine rich splicing factor 11; SYVN1, synoviolin 1; TFR2, transferrin receptor 2; TNC, tenascin C; TRAPPC6B, trafficking protein particle complex subunit 6B; VCP, valosin containing protein; XPOT, exportin for tRNA; HBB, hemoglobin subunit beta
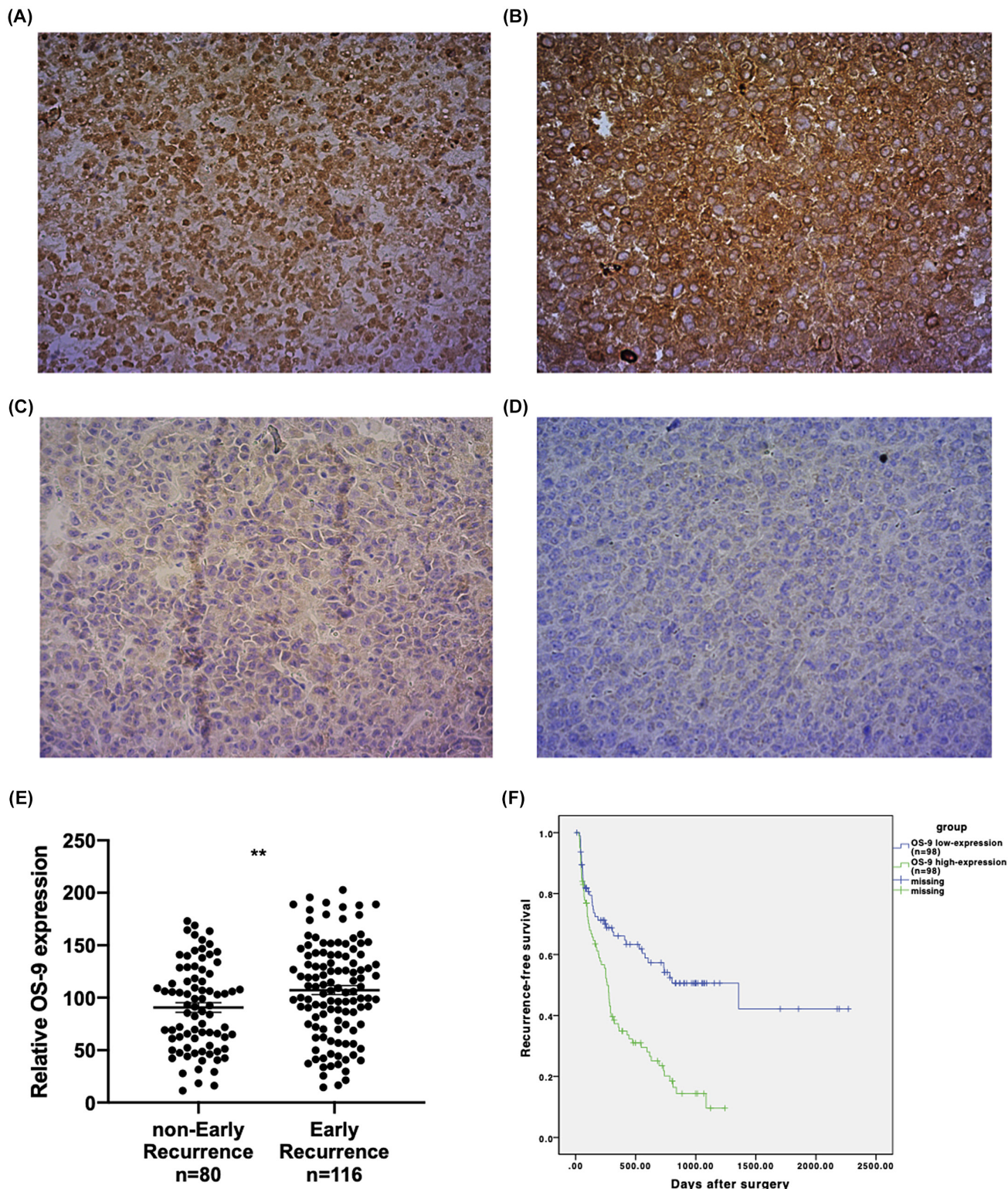
FIGURE 2 Correlations between OS-9 expression and HCC recurrence. (A,B) Representative immunohistochemistry (IHC) staining on surgical specimens of high OS-9 expression. (C,D) Representative IHC staining on surgical specimens of low OS-9 expression. (E) Scatter plot of the expression of OS-9 using histochemistry score of tumor tissues in both recurrence and nonrecurrence groups. Patients in the early recurrence group showed higher expression of OS-9 in the tumor tissue significantly ($p < 0.01$). (F) Recurrence-free survival of patients with HCC stratified by OS-9 expression, the high OS-9 expression in the tumor tissue group expressed significantly poor recurrence-free survival ($p < 0.001$)

TABLE 3 Relationship between the expression of OS-9 and the clinical characteristics of HCC patients

Feature	n	OS-9 high expression (n = 98)	OS-9 low expression (n = 98)	x^2	p value
Age				2.252	0.133
<60 years	128	59	69		
≥60 years	68	39	29		
Gender				0.040	0.841
Male	167	84	83		
Female	29	14	15		
Tumor size				3.207	0.073
1–10 cm	145	67	78		
>10 cm	51	31	20		
Histological differentiation				0.021	0.886
Well	105	52	53		
Poor	91	46	45		
Vascular invasion				0.749	0.186
No	121	56	65		
Yes	75	42	33		
Number of tumors				0.413	0.521
Solitary	171	87	84		
Multiple	25	11	14		
Serum AFP				6.382	0.012
<20 ng/ml	71	27	44		
≥20 ng/ml	125	71	54		
Recurrence				14.278	0.000
No	80	25	55		
Yes	116	73	43		

Abbreviation: AFP, alpha-fetoprotein.

TABLE 4 Relationship between the clinical characteristics and the recurrence of patients with hepatocellular carcinoma

	Univariate analysis			Multivariate analysis		
	p value	Hazard ratio	95% CI	p value	Hazard ratio	95% CI
Age (≥60 years)	0.027	0.636	0.426–0.951	0.017	0.608	0.405–0.914
Gender (male)	0.255	1.323	0.817–2.143			
Serum AFP (>20 ng/ml)	0.006	1.773	1.183–2.656	0.192	1.328	0.867–2.034
Tumor size (>10 cm)	0.000	4.008	2.695–5.960	0.000	3.107	2.032–4.751
Number of tumors (multiple)	0.618	1.145	0.673–1.946			
Pathological differentiation (poor)	0.000	1.970	1.365–2.843	0.010	1.631	1.123–2.369
Vascular invasion (yes)	0.000	2.470	1.708–3.573	0.037	1.531	1.026–2.285
0S-9 expression (high)	0.000	2.006	1.371–2.934	0.001	1.977	1.326–2.949

Abbreviation: CI, confidence interval.

OS-9 predicted poor overall survival in patients with HCC

Univariate and multivariate Cox analyses were performed to evaluate the prognostic factors for HCC recurrence Table 4). The univariate analysis revealed that patient age >60 years, serum AFP levels > 20 μg/l, tumor size > 10 cm, poor/medium-poor pathological differentiation, microvascular invasion, and high OS-9 expression were significant risk factors that could increase the recurrence rate in patients with HCC. The multivariate analysis showed that patient age > 60 years, tumor size > 10 cm, poor/medium-poor pathological differentiation, vascular invasion, and high OS-9 expression were significantly associated with tumor recurrence.
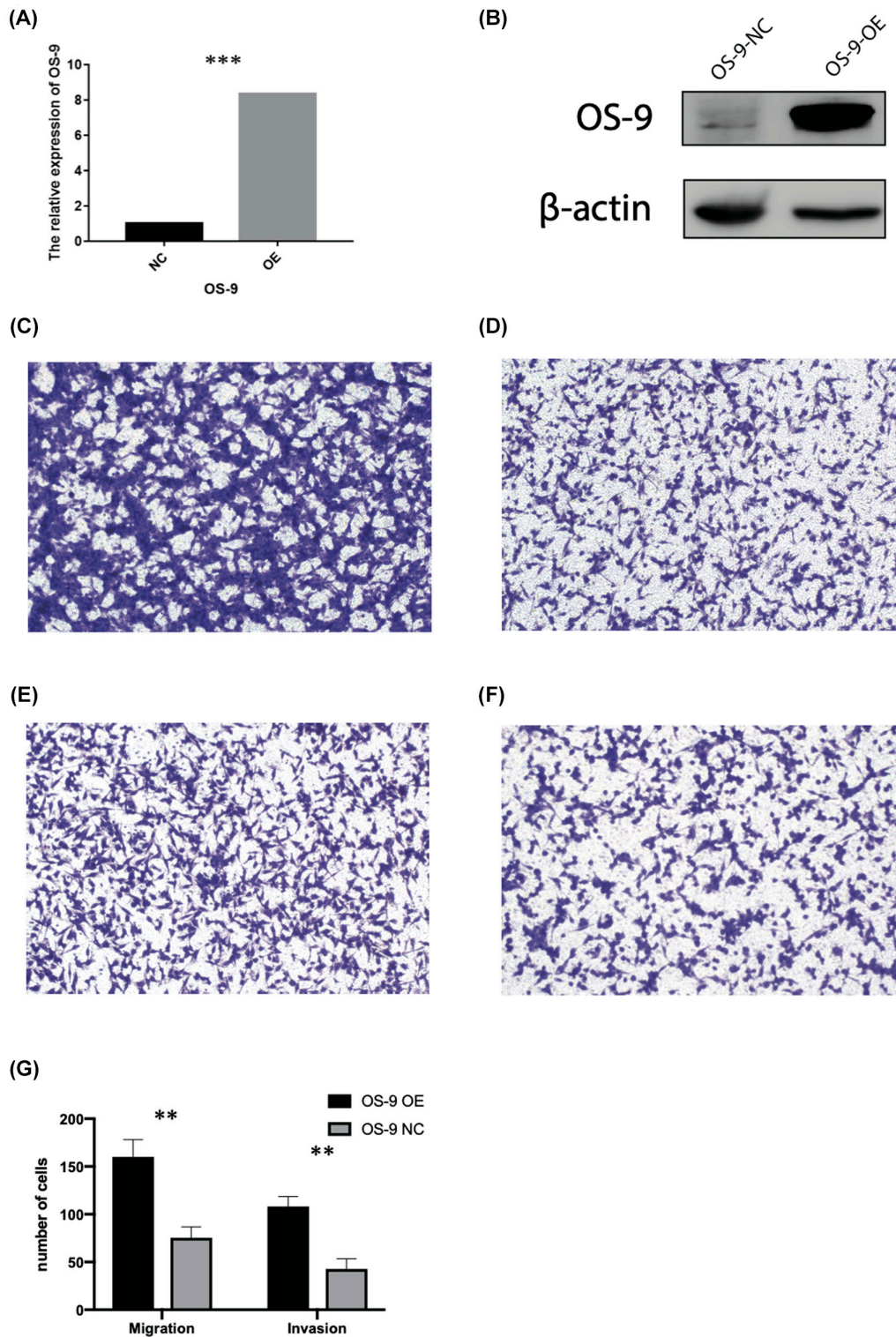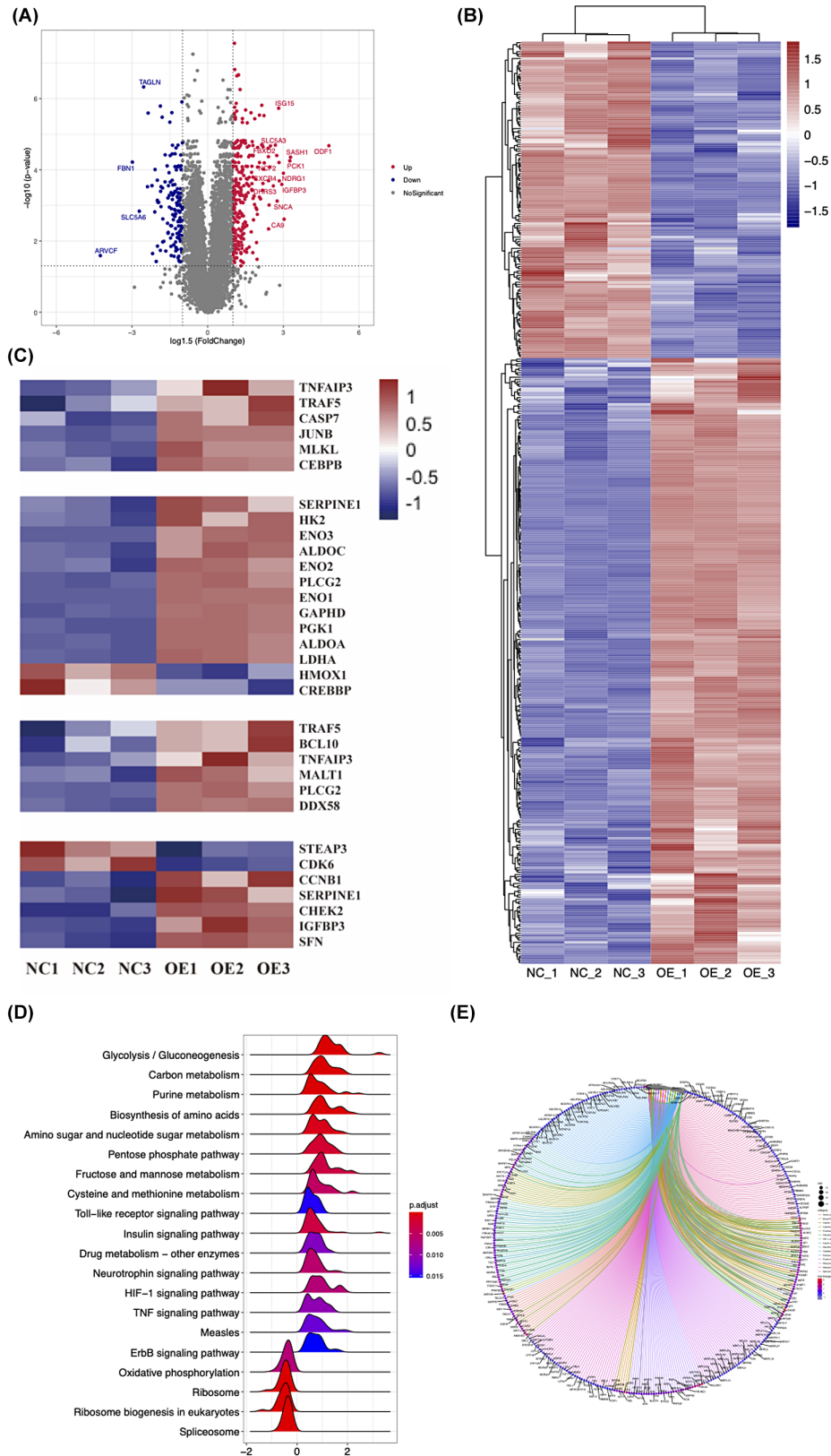
FIGURE 3　OS-9 promoted SMMC-7721 cell migration, and invasion. (A,B) OS-9 overexpression efficiency verification after lentiviruses transfection. (C) Effects of OS-9 overexpression group on cell migration capacity by Transwell assays in SMMC-7721 cells. (D) Effects of control group on cell migration capacity. (E) Effects of OS-9 overexpression group on cell invasion capacity. (F) Effects of control group on cell invasion capacity. (G) Results from Transwell assay revealed an increased migratory and invasion capacity of OS-9 overexpression SMMC-7721 cell lines ($p < 0.01$). Abbreviations: NC, control; OE, overexpressed

OS-9 promoted SMMC-7721 cell migration and invasion

In vitro assays were performed to explore the potential function of OS-9 in HCC cells. The overexpression of

OS-9 using lentiviruses was verified to be feasible in SMMC-7721 cells (Figure 3A,B). The transwell assay revealed the increased migratory (Figure 3C,D; *p* <0.01) and invasive (Figure 3E,F; *p* <0.01) capacity of SMMC-7721 cells with OS-9 overexpression.

FIGURE 4 Differential proteins expression in OS-9 overexpression group (n = 3) and vector control (n = 3) of SMMC-7721 cells. (A) Volcano plot of the differentially expressed proteins. Gray dots represent genes that are not differentially expressed in the early recurrence group and nonrecurrence group; red dots and blue dots represent genes that are up-regulated and down-regulated significantly in the early recurrence group. (B) Heat map of the differentially expressed proteins. Red rectangles mean that genes are up-regulated in these samples, and blue ones mean down-regulated. Two hundred and sixty-eight protein expressions were up-regulated and 140 protein expressions were down-regulated in the overexpression group compared with the vector control group (fold change ≥ 1.5; $p < 0.05$). (C) Heat map of the differentially expressed proteins classified to the hypoxia-inducible factor 1 (HIF-1) and tumor necrosis factor (TNF) signaling pathway. (D) Ridgeline plot of Kyoto Encyclopedia of Genes and Genomes pathway enrichment for differentially expressed proteins. (E) Gene Ontology functions for differentially expressed proteins. The left side of the circle includes all related genes, and the right side displays the Gene Ontology terms. Red and blue rectangles mean that genes are up-regulated and down-regulated in the early recurrence group. Abbreviations: ALDOA, aldolase, fructose-bisphosphate A; ALDOC, aldolase, fructose-bisphosphate C; BCL10, BCL10 immune signaling adaptor; CASP7, caspase 7; CCNB1, cyclin B1; CDK6, cyclin dependent kinase 6; CEBPB, CCAAT enhancer binding protein beta; CHEK2, checkpoint kinase 2; CREBBP, CREB binding protein; DDX58, DExD/H-box helicase 58; ENO1, enolase 1; ENO2, enolase 2; ENO3, enolase 3; HK2, hexokinase 2; HMOX1, heme oxygenase 1; IGFBP3, insulin like growth factor binding protein 3; JUNB, JunB proto-oncogene; LDHA, lactate dehydrogenase A; MALT1, MALT1 paracaspase; MLKL, mixed lineage kinase domain like pseudokinase; OE, overexpressed; PGK1, phosphoglycerate kinase 1; PLCG2, phospholipase C gamma 2; SERPINE1, serpin family E member 1; SFN, stratifin. NC, control; STEAP3, STEAP3 metalloreductase; TNFAIP3, TNF alpha induced protein 3; TRAF5, TNF receptor associated factor 5

Potential interacting proteins directly targeted by OS-9 in SMMC-7721 cells

To determine the molecular mechanisms by which OS-9 regulates HCC recurrence, MS was used. Potential interacting proteins were analyzed between SMMC-7721 cells with stable OS-9 overexpression and those with the vector control. The expression of 268 proteins was up-regulated, and that of 140 proteins was down-regulated, in the overexpression group compared with that in the vector control group (fold change ≥ 1.5; $p < 0.05$). Several significant proteins, including mixed lineage kinase domain-like (MLKL), tumor necrosis factor alpha–induced protein 3 (TNFAIP3), JunB proto-oncogene (JUNB), caspase-7 (CASP7), enolase1 (ENO1), enolase2 (ENO2), enolase3 (ENO3), and lactate dehydrogenase A (LDHA), were differentially expressed (Figure 4).

Functional classification of differentially expressed proteins by bioinformatic analysis

Based on the data shown previously, a systematic bioinformatic analysis (protein function annotation) was carried out to determine GO terms and KEGG pathways in which the differentially expressed proteins were significantly enriched. GO, KEGG, and protein domain analyses indicated the involvement of differentially expressed proteins and signaling pathways in regulation of the HIF-1 and TNF signaling pathways (Figure 4).

mRNA expression in the HIF-1 and TNF signaling pathways

OS-9 overexpression significantly promoted the expression of mRNAs involved in the HIF-1 and TNF signaling pathways in SMMC-7721 cells. The mRNA expression levels of *MLKL*, *TNFAIP3*, *JUNB*, *CASP7*, *TNF-α*, and tumor necrosis factor receptor–associated factor 6 (*TRAF6*) increased more than 2-fold in SMMC-7721 cells with OS-9 overexpression, which represented activation of the TNF signaling pathway. Moreover, the expression of *ENO1*, *ENO2*, *ENO3*, *LDHA*, and aldolase, fructose-bisphosphate A (*ALDOA*) was elevated by more than 3-fold in this group, indicating activation of the HIF-1 signaling pathway (Figure 5).

Interplay between HIF-1α or TNFα signaling pathway and OS-9

OS-9 overexpression significantly induced up-regulation of HIF-1 expression in SMMC-7721 cells by western blot results (Figure 6A,B). Transwell assay were also adopted in OS-9 overexpression and control SMMC-7721 cell line with or without HIF-1α or TNF-α inhibitors. The results showed that invasion and migration of OS-9 overexpressed cell line (Figure 6C,D) were weakened using HIF-1α inhibitor (Figure 6E,F). There are also significant changes for migration and invasion of OS-9 overexpressed HCC cell line using TNF-α inhibitor (Figure 6G,H)

DISCUSSION

Increasing evidence has demonstrated that proteins play important roles in the recurrence and metastasis of HCC, which is accompanied by changes in the expression patterns of various proteins. In this study, proteomics was performed using tumor specimens from early recurrence and nonrecurrence patients; the change in OS-9 expression exceeded 300-fold and was largest among all of the proteins investigated. Based on these results, more clinical samples were collected, and IHC analysis was performed to identify the critical
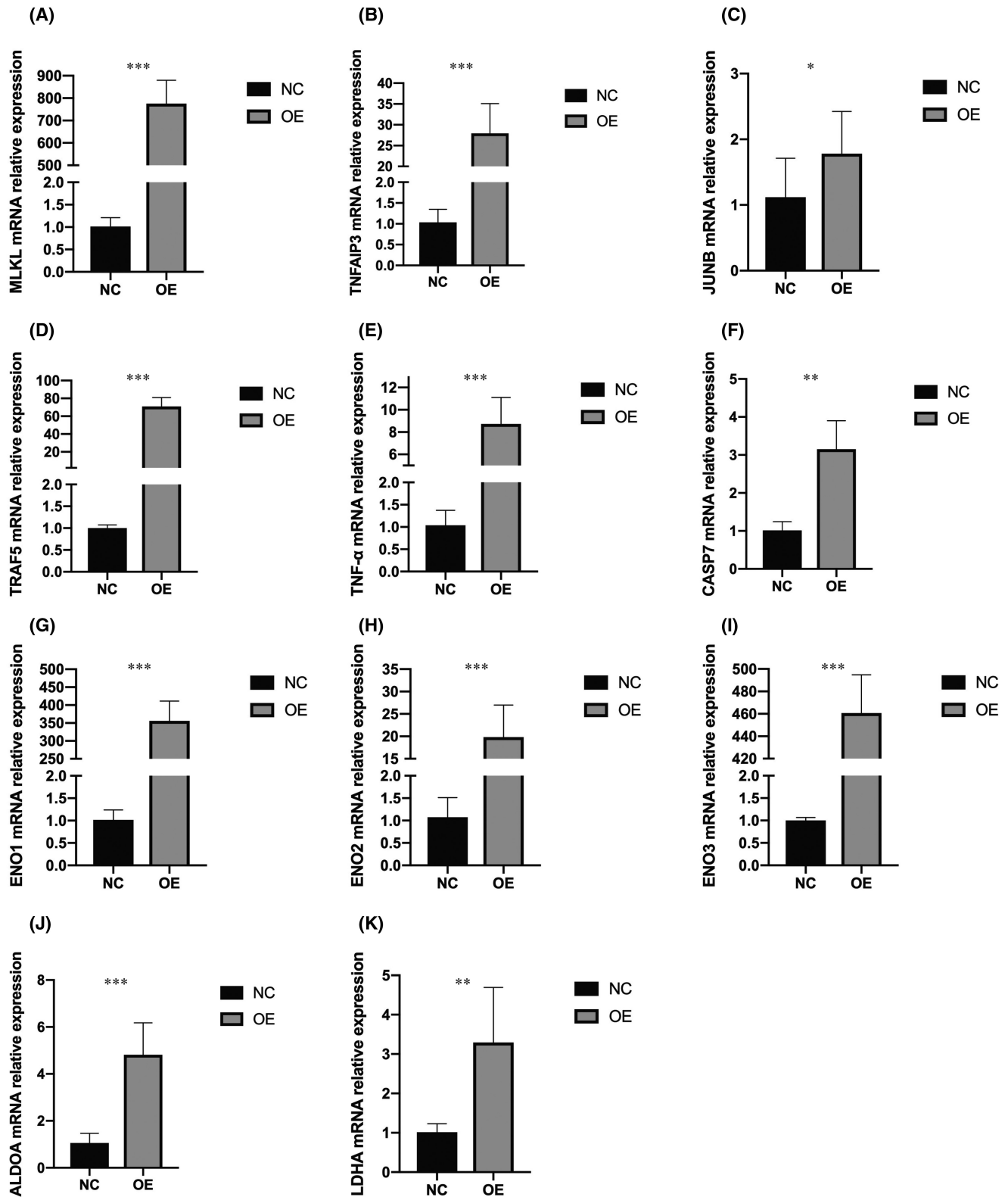
FIGURE 5 (A–K) The relative messenger RNA (mRNA) expression level of lineage kinase domain-like MLKL (A), tumor necrosis factor alpha–induced protein 3 (TNFAIP3) (B), JunB proto-oncogene (JUNB) (C), and tumor necrosis factor receptor–associated factor 5 (TRAF5) (D), TNF-α (E) and caspase-7 (CASP7) (F) could be observed to increase more than 2-fold ($p < 0.01$). The relative expression of enolase1 (ENO1) (G), enolase2 (ENO2) (H), enolase3 (ENO3) (I), aldolase, fructose-bisphosphate A (ALDOA) (J), and lactate dehydrogenase A (LDHA) (K) were also elevated more than 2-fold ($p < 0.01$)
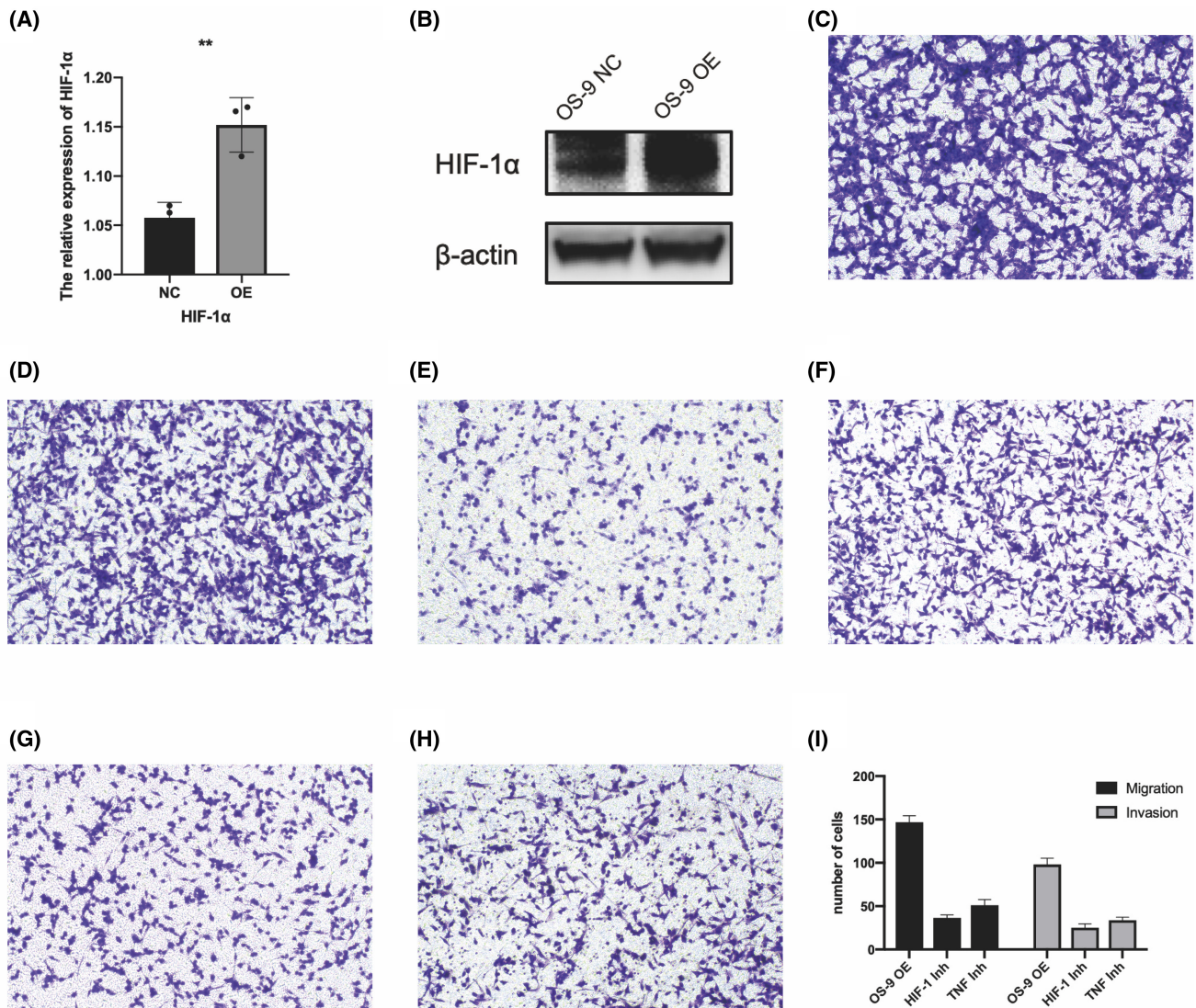
FIGURE 6 Interplay between HIF-1 or TNF signaling pathway and OS-9. (A,B) The expression of HIF-1α in OS-9 overexpression and control group was confirmed by western blot analysis. Results showed that OS-9 overexpression induced up-regulation of HIF1α expression with a ratio over 1.1 fold ($p < 0.01$). (C) Effects of OS-9 overexpression group on cell migration capacity by Transwell assays in SMMC-7721 cells. (D) Effects of OS-9 overexpression group on cell invasion capacity. (E) Effects of OS-9 overexpression group treated with HIF1α inhibitor (VH-298, 20 μM) on cell migration capacity. (F) Effects of OS-9 overexpression group treated with HIF1α inhibitor on cell invasion capacity. (G) Effects of OS-9 overexpression group treated with TNFα inhibitor (Methylthiouracil, 20 μM) on cell migration capacity. (H) Effects of OS-9 overexpression group treated with TNF-α inhibitor on cell invasion capacity. (I) Results from Transwell assay revealed a decreased migration or invasion capacity of OS-9 overexpression treated with HIF-1α or TNF-α inhibitor in SMMC-7721 cell lines ($p < 0.001$)

role of OS-9 in HCC tumor size and recurrence. OS-9 overexpression enhanced the migration and invasion capacities of SMMC-7721 cells. MS analysis demonstrated the correlation of proteins with OS-9, which was elevated in tumor tissues.

Progress has been made in treatment strategies for HCC; however, the recurrence-free survival of patients with HCC has not improved. Novel biomarkers are urgently needed to improve the prognosis of these patients. The function of OS-9, an endoplasmic reticulum lectin, in tumor regulation is rarely analyzed, and contradictory conclusions have been reached. Overexpression of OS-9 has been observed in osteosarcomas, and

OS-9 was reported to be co-amplified with CDK4 in three of five sarcoma tissues.[6] OS-9 acts as a part of the endoplasmic reticulum–associated degradation (ERAD) machinery and aids in the transfer of misfolded proteins.[11] Sun et al. discovered that the long noncoding RNA ENST00000480739 negatively regulates HIF-1α expression by up-regulating OS-9 expression in pancreatic ductal adenocarcinoma, and that the downregulation of HIF-1α expression through OS-9 indicates underlying tumor metastasis. However, no study has indicated a correlation between OS-9 and HCC. Numerous unfolded/misfolded proteins are degraded by ERAD, which is regarded as an important ER-folded

protein and plays an essential role in the maintenance of endoplasmic reticulum homeostasis.[12] ERAD has proven to be involved in plenty kinds of oncogenesis. The blocking of ERAD is sufficient to impair cancer stemness–emphasized endoplasmic reticulum proteostasis to the cancer stem cell and cancer development.[13] In addition, activating of ERAD could promote the cell survival and growth of HCC.[12,14] At present, there is no direct evidence that OS-9 works through ERAD to enhance the recurrence of HCC. However, we believe that OS-9, as an important protein of ERAD, should also play a role through this pathway.

Proteomic results showed that the expression of OS-9 in tumor tissues and adjacent normal tissues in patients with early recurrence was significantly higher than that in patients without recurrence. However, there is no difference of OS-9 expression between tumor tissue and adjacent normal tissue in the same group of patients. The verification of IHC staining on surgical specimens from 196 patients with HCC also confirmed these results. Nevertheless, we found the difference in fold change between tumor tissues was higher than that in adjacent normal tissues (histochemistry score: 118.73 vs. 68.28; $p < 0.001$). Although the "seeds" were removed by surgical resection, the remaining "soil" did not show a significant difference in OS-9 expression. We assumed that the condition was mediated by the extracellular matrix (ECM), which surrounds hepatocytes and creates a permissive soil after HCC recurrence. The injury is persistent in the context of chronic liver injury, regeneration, and cirrhosis; thereafter, the net accumulation of ECM remodeling results in a poor prognosis.[15]

IHC analysis was performed in 196 patients to validate the role of OS-9 in HCC progression. Categorized by median OS-9 expression based on IHC analysis, higher OS-9 levels were correlated with tumor size, serum AFP levels, and HCC recurrence. The multivariate Cox analysis showed that tumor size, pathological differentiation, vascular invasion, and OS-9 expression were significantly associated with tumor recurrence. The recurrence-free survival rate of patients with HCC with high expression of OS-9 was far lower than that of patients with low expression of OS-9, suggesting that the high expression of OS-9 is an important adverse prognostic factor for HCC, which is consistent with our result that the high expression of OS-9 was positively correlated with the size of HCC tumors and AFP levels. This indicates that the high expression of OS9 may be involved in the occurrence and development of HCC and is a crucial adverse prognostic factor for HCC. Based on *in vitro* experiments, we determined that the overexpression of OS-9 could enhance the invasion and migration of SMMS-7721 cells.

The mass spectrum showed that OS-9 interacted with 408 cellular proteins, most of which were located in the nucleus and cytoplasm, as determined using the UniProt database, indicating the various functions of OS-9 in regulating cellular activity and molecular function. To determine GO terms and KEGG pathways in which the differentially expressed proteins are significantly enriched, we carried out the following three enrichment analyses: GO classification, KEGG pathway, and protein domain. GO functional enrichment analysis of differentially expressed genes showed that the up-regulated genes in HCC cells were primarily involved in monosaccharide catabolic/biosynthetic and peptidase regulator activity–related processes, and the down-regulated genes were primarily involved in the biological processes of calcium ion binding or protein complex binding. KEGG analysis showed that the expression of OS-9 regulated the development of HCC. The overexpression of OS-9 was related to up-regulation of the HIF-1 and TNF signaling pathways. However, the regulation of proteins related to microRNAs (miRNAs) in cancer cells and the Wnt signaling pathway was also observed in the raw data of our proteomics results.

The transcription of HIF-1 has been shown to activate a wide repertoire of genes that promote tumor growth and metastasis and is associated with poor clinical outcomes. HIF-1 can regulate the expression of various target genes and promote hypoxia, which activates the transcription of genes responsible for angiogenesis, glucose metabolism, proliferation, invasion, and metastasis in HCC.[16–18] Moreover, HIF-1 is a particularly crucial protein for shifting the metabolic program from oxidative phosphorylation to glycolysis, and its expression was up-regulated in SMMS-7721 cells with OS-9 overexpression in our study.[16] The potential role of HIF-1α in the barrier-modulation function of OS-9 was determined by Sun et al.; however, HIF-1α levels were not affected by OS-9 overexpression or direct physical interaction in this study.[19] Similarly, we observed activation of the HIF-1 signaling pathway rather than overexpression of the HIF-1 protein. The expression of ENO1, ENO2, ENO3, ALDOA, and LDHA was more than 2-fold higher in the OS-9 overexpression group.

TNF-α has been revealed to be a vital cytokine for tumor progression, as well as apoptosis, inflammation, and immunity, and is produced and released by activated macrophages.[20] Zhao et al. revealed that TNF-α inhibits the expression of miR-497 and promotes the self-renewal and metastasis phenotypes of HCC cells through the nuclear factor kappa B (NF-κB)/miR-497/SALL4 axis, which is associated with poor prognosis in patients with HCC.[21] The knockdown of TNF-α could inhibit the activation and proliferation of hepatic progenitor cells through the tumor necrosis factor receptor 2 (TNFR2)/signal transducer and activator of transcription 3 signaling pathway to inhibit hepatocellular carcinogenesis.[22] Two distinct surface receptors were discovered: TNFR1 and TNFR2. An extensive cross-talk among the apoptosis, NF-κB, and JNK signaling pathways generated from TNFR1, which initiates most of the biological activities of TNF-α, has been confirmed.[23] Ligand

binding to TNFR2 could lead to activation of the NF-κB, p38 mitogen-activated protein kinase, extracellular signal–regulated kinase, and phosphatidylinositol 3-kinase pathways, which are related to cell proliferation, migration, and survival and the modulation of regulatory T-cell function.[23,24] In our study, TNFAIP3, JUNB, CASP7, TNF-α, and TRAF5 expression was more than 2-fold higher in the OS-9 overexpression group; this indicates that the expression of these proteins serves as a biomarker in human HCC tissues. Furthermore, elevated TNFAIP3 levels can lead to oncogenic properties.[25,26] To further examine the interplay between HIF1-α or TNF and OS-9, inhibitors of these two pathways were adopted. The Transwell array results revealed that the overexpression of OS-9 could enhance the migration and invasion capacity of the HCC cell line, blocking the two proteins prevented OS-9 from inducing migration and invasion in HCC where OS-9 is overexpressed.

In conclusion, the results of our study suggest the effect of OS-9 on the tumorigenesis, development, and adverse prognosis of HCC. A higher OS-9 expression is related to higher AFP levels and leads to a lower recurrence-free survival rate. The overexpression of OS-9 enhances the invasion and migration of SMMS-7721 cells. According to MS, GO, and KEGG analyses, the HIF-1 and TNF signaling pathways are activated in tumor cells with OS-9 overexpression. The expression of various key proteins in these pathways is significantly changed. This study provides a potential protein biomarker that could help improve the prognosis and recurrence-free survival of patients with HCC after surgery.

CONFLICT OF INTEREST
Nothing to report.

AUTHOR CONTRIBUTIONS
Data management, statistical analysis, and manuscript draft: Xuyong Wei and Mengfan Yang. *Cohort identification, experimental implementation, and data management:* Binhua Pan, Xiaobing Zhang, Hanchao Lin, Wangyao Li, Wenzhi Shu, Kun Wang, Abdul Rehman Khan, Xuanyu Zhang, and Beini Cen. *Project administration:* Xiao Xu performed. All authors searched the literature, designed the study, interpreted the findings, and revised the manuscript.

ORCID
Xiao Xu https://orcid.org/0000-0002-2761-2811

REFERENCES

1. Siegel RL, Miller KD, Jemal A. Cancer statistics, 2020. CA Cancer J Clin. 2020;70:7–30.

2. Jiang JW, Chen XH, Ren Z, Zheng SS. Gut microbial dysbiosis associates hepatocellular carcinoma via the gut-liver axis. Hepatobiliary Pancreat Dis Int. 2019;18:19–27.

3. Wu J-C, Huang Y-H, Chau G-Y, Su C-W, Lai C-R, Lee P-C, et al. Risk factors for early and late recurrence in hepatitis B-related hepatocellular carcinoma. J Hepatol. 2009;51:890–7.

4. Zhang YI, Tao R, Wu S-S, Xu C-C, Wang J-L, Chen J, et al. TRIM52 up-regulation in hepatocellular carcinoma cells promotes proliferation, migration and invasion through the ubiquitination of PPM1A. J Exp Clin Cancer Res. 2018;37:116.

5. Xie Y, Du J, Liu Z, Zhang D, Yao X, Yang Y. MiR-6875-3p promotes the proliferation, invasion and metastasis of hepatocellular carcinoma via BTG2/FAK/Akt pathway. J Exp Clin Cancer Res. 2019;38:7.

6. Su YA, Hutter CM, Trent JM, Meltzer PS. Complete sequence analysis of a gene (OS-9) ubiquitously expressed in human tissues and amplified in sarcomas. Mol Carcinog. 1996;15:270–5.

7. Kimura Y, Nakazawa M, Yamada M. Cloning and characterization of three isoforms of OS-9 cDNA and expression of the OS-9 gene in various human tumor cell lines. J Biochem. 1998;123:876–82.

8. Baek JH, Mahon PC, Oh J, Kelly B, Krishnamachary B, Pearson M, et al. OS-9 interacts with hypoxia-inducible factor 1alpha and prolyl hydroxylases to promote oxygen-dependent degradation of HIF-1alpha. Mol Cell. 2005;17:503–12.

9. Sun YW, Chen YF, Li J, Huo YM, Liu DJ, Hua R, et al. A novel long non-coding RNA ENST00000480739 suppresses tumour cell invasion by regulating OS-9 and HIF-1α in pancreatic ductal adenocarcinoma. Br J Cancer. 2014;111:2131–41.

10. Yu L, Nian Z, Sang J. Osteosarcoma amplified 9 is highly expressed in mouse adipocytes and controls lipid storage. Mol Med Rep. 2011;4:687–92.

11. Martin BL, Conley SM, Harris RS, Stanley CD, Niyitegeka JM, Ongeri EM. Hypoxia associated proteolytic processing of OS-9 by the metalloproteinase meprin β. Int J Nephrol. 2016;2016:2851803.

12. Liu Y, Tao S, Liao L, Li Y, Li H, Li Z, et al. TRIM25 promotes the cell survival and growth of hepatocellular carcinoma through targeting Keap1-Nrf2 pathway. Nat Commun. 2020;11:348.

13. Li C, Huang Y, Fan Q, Quan H, Dong Y, Nie M, et al. p97/VCP is highly expressed in the stem-like cells of breast cancer and controls cancer stemness partly through the unfolded protein response. Cell Death Dis. 2021;12:286.

14. Gong J, Fang L, Liu R, Wang Y, Xing J, Chen Y, et al. UPR decreases CD226 ligand CD155 expression and sensitivity to NK cell-mediated cytotoxicity in hepatoma cells. Eur J Immunol. 2014;44:3758–67.

15. Wu XZ, Chen D, Xie GR. Extracellular matrix remodeling in hepatocellular carcinoma: effects of soil on seed? Med Hypotheses. 2006;66:1115–20.

16. Kung-Chun Chiu D, Pui-Wah Tse A, Law C-T, Ming-Jing Xu I, Lee D, Chen M, et al. Hypoxia regulates the mitochondrial activity of hepatocellular carcinoma cells through HIF/HEY1/PINK1 pathway. Cell Death Dis. 2019;10:934.

17. Wong CC, Kai AK, Ng IO. The impact of hypoxia in hepatocellular carcinoma metastasis. Front Med. 2014;8:33–41.

18. Chen Y, Huang F, Deng L, Yuan X, Tao Q, Wang T, et al. HIF-1-miR-219-SMC4 regulatory pathway promoting proliferation and migration of HCC under hypoxic condition. Biomed Res Int. 2019;2019:8983704.

19. Sun L, Xu C, Chen G, Yu M, Yang S, Qiu Y, et al. A novel role of OS-9 in the maintenance of intestinal barrier function from hypoxia-induced injury via p38-dependent pathway. Int J Biol Sci. 2015;11:664–71.

20. Ma W, Chen XI, Wu X, Li J, Mei C, Jing W, et al. Long noncoding RNA SPRY4-IT1 p	romotes proliferation and metastasis of hepatocellular carcinoma via mediating TNF signaling pathway. J Cell Physiol. 2020;235:7849–62.

21. Zhao B, Wang Y, Tan X, Ke K, Zheng X, Wang F, et al. Inflammatory micro-environment contributes to stemness properties and metastatic potential of HCC via the NF-κB/miR-497/SALL4 axis. Mol Ther Oncolytics. 2019;15:79–90.

22. Jing Y, Sun K, Liu W, Sheng D, Zhao S, Gao L, et al. Tumor necrosis factor-alpha promotes hepatocellular carcinogenesis through the activation of hepatic progenitor cells. Cancer Lett. 2018;434:22–32.

23. Chen G, Goeddel DV. TNF-R1 signaling: a beautiful pathway. Science. 2002;296:1634–5.

24. Lebrec H, Ponce R, Preston BD, Iles J, Born TL, Hooper M. Tumor necrosis factor, tumor necrosis factor inhibition, and cancer risk. Curr Med Res Opin. 2015;31:557–74.

25. Chen H, Hu L, Luo Z, Zhang J, Zhang C, Qiu B, et al. A20 suppresses hepatocellular carcinoma proliferation and metastasis through inhibition of Twist1 expression. Mol Cancer. 2015;14:186.

26. Wang X, Ma C, Zong Z, Xiao Y, Li N, Guo C, et al. A20 inhibits the motility of HCC cells induced by TNF-α. Oncotarget. 2016;7:14742–54.